Tunable thermal conductivity in mesoporous silicon by slight porosity change

Jae Hun Seol, David S. Barth, Jia Zhu, Dušan Ćoso, Kedar Hippalgaonkar, Jongwoo Lim, Junkyu Han, Xiang Zhang, and Arun Majumdar

Citation: Appl. Phys. Lett. **111**, 063104 (2017); doi: 10.1063/1.4997747

View online: http://dx.doi.org/10.1063/1.4997747

View Table of Contents: http://aip.scitation.org/toc/apl/111/6

Published by the American Institute of Physics

Tunable thermal conductivity in mesoporous silicon by slight porosity change

Jae Hun Seol,[1,a)] David S. Barth,[2] Jia Zhu,[2] Dušan Ćoso,[3] Kedar Hippalgaonkar,[4] Jongwoo Lim,[5] Junkyu Han,[1] Xiang Zhang,[2] and Arun Majumdar[3,a)]
[1]*School of Mechanical Engineering, Gwangju Institute of Science and Technology (GIST), Buk-gu, Gwangju 61005, South Korea*
[2]*Department of Mechanical Engineering, University of California at Berkeley, Berkeley, California 94720, USA*
[3]*Department of Mechanical Engineering & Precourt Institute for Energy, Stanford University, Stanford, California 94305-4240, USA*
[4]*Institute of Materials Research and Engineering, A*Star (Agency for Science, Technology and Research), 2 Fusionopolis Way, Innovis, 08-03, 138634 Singapore*
[5]*Department of Chemistry, Seoul National University, Seoul 08826, South Korea*

(Received 10 April 2017; accepted 18 July 2017; published online 8 August 2017)

We report the thermal conductivity of photoelectrochemically synthesized mesoporous silicon (MPS), with ~20-nm diameter pores and 52%–58% porosity. The thermal conductivity of MPS samples with a thickness of a few microns was measured using the three omega (3ω) differential technique. We experimentally demonstrated that the thermal conductivity of MPS varies between 3 and 7 W/m K at room temperature and is dependent on the photoelectrochemical etching times used during the MPS synthesis, which induces a slight change in the MPS porosity. Calculations were conducted using the Boltzmann transport equation in the relaxation time approximation, with the results suggesting that the large thermal conductivity reduction in the MPSs was not entirely explained by the pore boundary scattering. Our findings indicate that elastic softening in the mesoporous structure may be responsible for the reduction in the thermal conductivity. *Published by AIP Publishing.* [http://dx.doi.org/10.1063/1.4997747]

Although silicon (Si) is the material of choice in the semiconductor industry, its application to light emission/absorption or optoelectronic devices has been limited due to its indirect bandgap that results in a low light-emission/absorption efficiency. However, porous Si has attracted considerable attention and has emerged as a rising candidate for such applications because of a report by Cullis and Canham showing that quantum confinement modifies the Si band structure, thereby enhancing the light-absorption/emission efficiency at the nanoscale.[1]

To facilitate the above applications, understanding of the thermal conductivity (k) of porous Si is crucial because the temperatures of optoelectronic devices are directly linked to their luminous efficacy.[2] Further, porous Si is regarded as a promising thermoelectric material with a potentially high thermoelectric figure of merit, i.e., $ZT \equiv \frac{\sigma S^2}{k} T$, where S, σ, and T are the Seebeck coefficient, the electrical conductivity, and the absolute temperature, respectively. Although the Si power factor σS^2 is sufficiently high, its high k has hindered the use of Si in thermoelectric applications. However, since Hochbaum *et al.*[3] demonstrated that the k value of Si nanowires with roughened surfaces can be lower than the Casimir limit,[4] various Si nanomaterials including porous Si have attracted considerable attention.[5–7] Numerous experimental[8–14] and theoretical[15–20] studies on the thermal properties of porous Si have been conducted. The measured k values have been shown to be reduced by as much as two orders of magnitude when the porosity (ε) is higher than 64%, which is attributed to the decrease in the phonon mean free path (MFP) confined by the porous structure.[9] Besides the k value of porous Si,[12] other thermoelectric properties, i.e., σ and S, of nanoscale porous Si have been measured and calculated.[21–23] In particular, the ZT value of optimally doped porous Si has been found to be larger than that of bulk Si.[22]

In this study, the effective k (k_{eff}) values of mesoporous silicon (MPS) samples with different porosities are measured in order to explore a mechanism of the k_{eff} reduction in MPS, which can be useful for optoelectronic and thermoelectric applications. Further, analysis is conducted using the phonon Boltzmann transport equation in the relaxation time approximation so as to estimate the phonon boundary scattering effect on the k_{eff} reduction.

To prepare the samples, MPS was synthesized using a simple and scalable process. A p-type Si wafer with a resistivity of 0.01–0.02 Ω cm was secured in a Teflon container etch bath filled with a 1:3 hydrofluoric acid (HF) and ethanol mixture. An MPS thin film was formed via etching under a constant current density of 3.53 mA/cm^2 and a light illumination of 450 W/m^2. Illumination decreased the porosity of p-type Si and worked for tuning the refractive index of MPS without having to apply a significantly low current density.[24,25] The pore size and spacing of porous Si are determined by several etching conditions, such as the ethanoic HF concentration, the current density, the doping type, and the doping concentration.[26] Here, the increased doping concentration transforms the pore shape from equiaxed to columnar.[27]

In the present study, cylindrical pores formed [Fig. 1(a)] as the MPS was synthesized from a heavily doped p-type wafer. In addition, branching pores stemming from the

a)Authors to whom correspondence should be addressed: jhseol@gist.ac.kr and amjumdar@stanford.edu

cylindrical pores appeared under low current density conditions, i.e., below 10 mA/cm^2.[28,29] The cylindrical pore sizes were measured using high-resolution scanning electron microscopy [SEM; Fig. 1(b)]. The average pore size was obtained to be approximately 21 nm; thus, the synthesized samples were categorized as MPS, i.e., porous Si with 10–50 nm pores.[30] Three MPS groups with thicknesses of approximately 1, 2, and 3 μm were synthesized by employing etching times of 4, 8, and 12 min, respectively (Table I). The ε values were determined using a Fourier transform infrared (FTIR) spectrometer, which provides a comparable measurement accuracy to that of the gravimetric method for the porosities around 50%.[31] The total reflectance values (R) of the MPS films were measured using varying light wavelengths. From the measured R, the refractive index of each porous Si film (n_{pSi}) was extracted (supplementary material). Note that the n_{pSi} value of a porous Si film, which is a function of ε, is expressed as

$$n_{pSi}(\varepsilon) = n_{Si}\sqrt{\left(2\varepsilon+2\right)\left(n_{Si}+n_{air}\right)^2 + \frac{(1-\varepsilon)\left(n_{Si}^4+n_{air}^4\right)}{(1+\varepsilon)n_{Si}^2+(1-\varepsilon)n_{air}^2}}, \quad (1)$$

where n_{Si} and n_{air} are the refractive indices of Si and air, respectively.[14,15] The ε values of the approximately 1, 2, and 3–μm-thick MPSs were measured to be 52, 57, and 58%, respectively. The tendency of ε to increase with the increasing etching time is related to the inhomogeneity of the pore size along the thickness direction.[32] As the etching proceeds, the pore size increases because of the gradual decrease in the ethanoic HF concentration. Further, the nonlinear trend of ε with respect to etching time agrees with the result of a previous report.[26]

To measure the k_{eff} values of the MPS films, the three-omega (3ω) differential method was employed. As shown in Fig. 1(a), an aluminum oxide (Al_2O_3) film of approximately

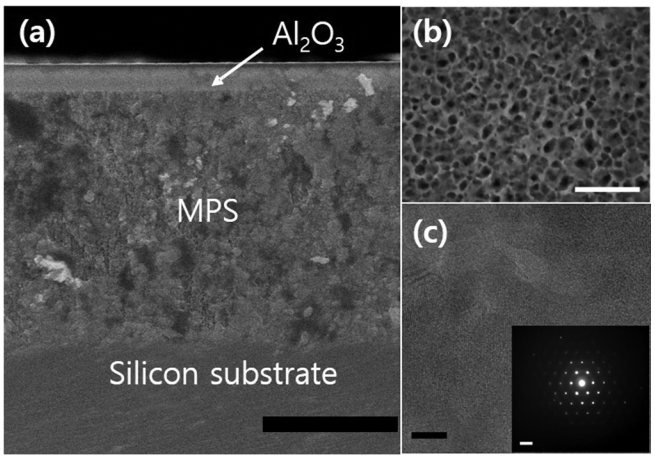

FIG. 1. (a) Scanning electron microscopy (SEM) cross-sectional image of the measurement device with the MPS film having 57% ε, synthesized from the heavily doped p-type Si wafer. The top-most layer is an Al_2O_3 film deposited on the MPS film via ALD. (b) High resolution SEM image of the top MPS surface. The pore size is approximately 30 nm. (c) Scanning transmission electron microscopy (STEM) images of MPS having identical ε. The inset shows the MPS diffraction pattern. Scale bars: (a)–(c) 1 μ m, 100 nm, and 10 nm, respectively; [(c), inset] 2 1/nm.

TABLE I. Etching times and Al_2O_3 and Pt thicknesses of MPS samples.

Sample	1	2	3	4	5	6	7
Etching time (min)	2	4	4	6	6	2	4
Porosity (%)	52	57	57	58	58	52	57
MPS thickness (μm)	0.99	2.05	2.11	2.94	3.06	1.35	2.54
Al_2O_3 thickness (nm)	…	250	253	250	253	230	230
Blocking Pt thickness (nm)	…	…	…		…	30	30

250-nm-thick was deposited via atomic layer deposition (ALD), which served as electrical insulation between the MPS layer and the platinum (Pt)/chromium (Cr) metal strip. Note that ALD is expected to provide a high quality interface, which is almost perfectly conformal to the MPS surface, thereby rendering the interface thermal resistance negligible. In addition to a relatively low deposition temperature of ~300 °C, there was a purging nitrogen gas in the ALD deposition chamber, which prevented the MPSs from being oxidized. Moreover, an ultra-thin Al_2O_3 layer could serve as an oxidation barrier.[33] However, penetration of the ALD precursors through the pores during deposition is of concern. Such penetration may fill the pores, yielding an increase in the measured k_{eff}. To address this issue, two different device batches were prepared, with (samples 1–5) and without (samples 6 and 7) an additional 30-nm-thick Pt layer sandwiched between the dielectric and the MPS film. Because the Pt layer thickness was larger than the pore size, the assumption that the Pt layer precluded the precursors from penetrating the porous film was justified. The k_{eff} values for these two sample batches are compared in the next paragraph. Finally, even if nanometer scale cracks originating from the thermal expansion coefficient mismatch between Al_2O_3, Pt, and MPS existed, they were likely rapidly filled with Al_2O_3 before a significant degree of penetration occurred.[34] Once Al_2O_3 was deposited, 210-nm-thick, 80–μm-long, and 20–μm-wide Pt/Cr metal strips were fabricated on top of the dielectric layer using standard photolithography techniques. The Pt and Cr thicknesses were 200 and 10 nm, respectively. Concurrently, an MPS-free reference measurement device was prepared, in order to apply the 3ω differential method.

The k_{eff} measurements were performed in a cryostat at pressures lower than 10^{-5} Torr. Figure 2 shows the measured cross plane k_{eff} of the MPS samples as a function of temperature. It is apparent that the k_{eff} value decreased with the increasing etching time (indicated in Table I for each sample). Further, the k_{eff} values of the 4 and 6 min etched samples are lower than those of the 2 min etched samples by 26% and 40% on average, respectively. Moreover, the k_{eff} values of samples 6 and 7, which have ~30-nm-thick Pt layers for adopting the 3ω differential method, are almost identical to those of their counterparts without the additional Pt layers. The same Pt layers were deposited for the reference samples of samples 6 and 7 as well for adopting the 3ω differential method. This indicates that the Al_2O_3 deposition in the pores did not significantly affect the k_{eff} value of the MPS films possibly because of the spontaneous surface blocking of the Al_2O_3 deposition. Additionally, as shown in Fig. S2, the measured k values of the substrates and Al_2O_3

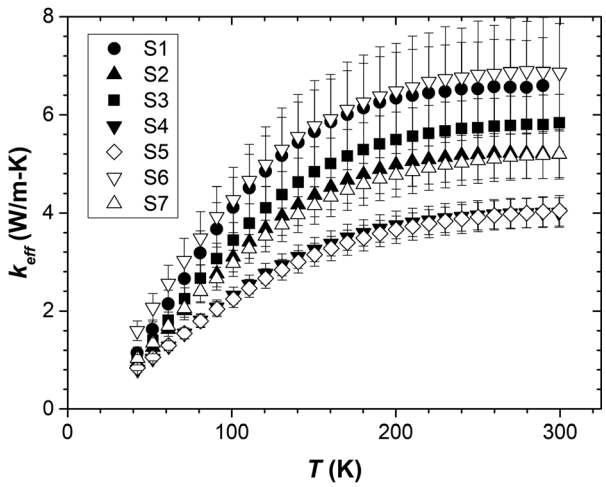

FIG. 2. MPS sample k_{eff} as a function of temperature. The k_{eff} values of 2- and 3-μm-thick MPSs are lower than that of the 1-μ m-thick MPSs by approximately 26% and 40%, respectively, at room temperature.

layers were compared with the values reported in the literature (supplementary material),[35,36] confirming the accuracy of our measurement results. When the MPS ε was higher than 60%, the measured k_{eff} value was inconsistent or the MPS layers tended to detach from the substrates easily. This may have been due to the structural fragility of MPS or the imperfect interface between the MPS and the subsequently deposited dielectric layer. After the thermal measurements, the thicknesses of the dissected MPSs were measured at several different positions near the 3ω metal strips using SEM as shown in Fig. S3. The averaged thicknesses are listed in Table I, and the relative standard deviation of the thicknesses was approximately 2% on average.

In order to gain a better understanding of the observed data shown in Fig. 2, the intrinsic k (k_{itrs}) values of the MPS samples were calculated using the phonon Boltzmann transport equation using the relaxation time approximation[37]

$$k_{itrs} = \frac{1}{3}\sum_{j=\mathrm{L},T,TU} v_j^2 \int_0^{\theta_j/T} C_{V,j}(x_\omega)\tau_j(x_\omega)dx_\omega, \qquad (2)$$

where j, θ, C_V, v, τ, and x are the polarization, the Debye temperature, the volumetric specific heat, the phonon group velocity, the relaxation time, and the non-dimensional frequency $x_c \equiv \frac{\hbar\omega}{kT}$, respectively. Corresponding to j, subscripts L, T, and TU represent the longitudinal and low and high frequency transverse phonon branches, respectively. The relaxation times for the phonon branches were estimated to be $\tau_L^{-1} = (A\omega^4 + B_L\omega^2T^3)$, $\tau_T^{-1} = (A\omega^4 + B_T\omega T^4)$, and $\tau_{TU}^{-1} = B_{TU}\omega^2/\sinh(x_\omega)$.[37,38] In these expressions, the fitting parameter A is the sum of the coefficients involved in the isotope ($A_{isotope}$), the mass difference between Boron and Si ($A_{\delta M}$), and the strain contributions ($A_{\delta R}$) such that $A = A_{isotope} + A_{\delta M} + A_{\delta R}$. Further, the fitting parameters B_L, B_T, and B_{Tu} contribute to three-phonon scattering, i.e., the normal and Umklapp processes. Considering the substrate doping concentration of 3.5 $\times 10^{18}$ cm^{-3}, $A_{isotope}$, $A_{\delta M}$, and $A_{\delta R}$ were adjusted to 1.98 $\times 10^{-45}$, 1.75 $\times 10^{-46}$, and 8.86 $\times 10^{-46}$, respectively.[38] Regardless of the doping concentration, B_L, B_T, and B_{TU} were taken to be 2 $\times 10^{-24}$, 9.3 $\times 10^{-13}$, and 5.5 $\times 10^{-18}$, respectively, which are identical to those used in a previous study.[39] From this scattering time calculation, the spectral $k_{intr,j}(\omega)$ of bulk Si for j polarization was obtained as

$$k_{itrs,j}(\omega) = \frac{1}{3}v_j^2 C_{V,j}(\omega)\tau_j(\omega) = \frac{1}{3}v_j C_{V,j}(\omega)\lambda_{0,j}(\omega), \qquad (3)$$

where $\lambda_{0,j}(\omega)$ ($\equiv \tau_j(\omega)v_j$) is the spectral MFP for j polarization. The overall k_{itrs} value was obtained by integrating the $k_{itrs,j}(\omega)$ value over the frequency range for each polarization and adding the respective $k_{itrs,j}$ contributions, originating from the different polarizations. In order to compare the calculation results with the measurement values, which were the k_{eff} values, the calculated k_{itrs} values were multiplied by a factor of $(1-\varepsilon)$, i.e., a material removal factor.[20]

As a result of the nanometer scale porous structure, the MFP was reduced by boundary scattering at the pore surfaces. This MFP reduction was integrated into the intrinsic bulk MFP based on Matthiessen's rule as proposed by Liu, and Asheghi proposed for calculating the k value of a thin Si film.[39] First, the MPS was assumed to have cylindrical pores because heavily doped Si produced a columnar structure.[27] The MFP reduction caused by the cylindrical boundaries was then analytically calculated following Hua and Cao (supplementary material).[20] Note that the phonons were diffusely scattered by the cylindrical pore boundaries, considering the rough surfaces of the MPS. Additionally, the MFP reduction caused by the limited thickness of the MPS film was calculated to be three quarters of the film thickness.[40] All these reducing factors were incorporated into the total MFP based on Matthiessen's rule. While Hua and Cao employed a single MFP value regardless of the phonon angular frequency (ω),[20] in the present work a frequency and polarization dependent relaxation time was applied based on the Holland model.[37] (A more detailed procedure is introduced in the supplementary material.) According to this analysis, the calculated k_{eff} values exhibited a stronger temperature dependence than the measured k_{eff} values as shown in Fig. 3(a). It was thought that long MFPs at low temperatures were strongly confined by the branching pores derived from the major cylindrical pores.

Therefore, a model with hexagonally ordered round pores was introduced to incorporate the phonon scattering by the branching pores stemming from the cylindrical pores. The reduced spectral MFP ($\lambda_j'(\omega)$), yielded by the hexagonally ordered round pores, was calculated as $\lambda_j'(\omega) = \lambda_{0,j}(\omega)/\left(1 + 4\lambda_{0,j}(\omega)/3l'\right)$.[40] Here, l' is the smallest distance between the adjacent pores, i.e., $l' = l\left(1 - \sqrt{\frac{2\sqrt{3}}{\pi}\varepsilon}\right)$, where l is the inter-pore spacing. l was taken to be 30 nm based on the high resolution SEM measurement of the inter-pore spacings. Note that the above equations assume that the reduced MFP was determined by the smallest thickness between the hexagonally ordered round pores. Therefore, the estimation, yielded by this model, provides the minimum k_{eff} value for the corresponding ε. The two different models, having cylindrical and round pores, respectively, encompass the k_{eff} values of columnar MPS obtained from the previous reports[8,10,13] as well as this study [Fig. 3(b)].

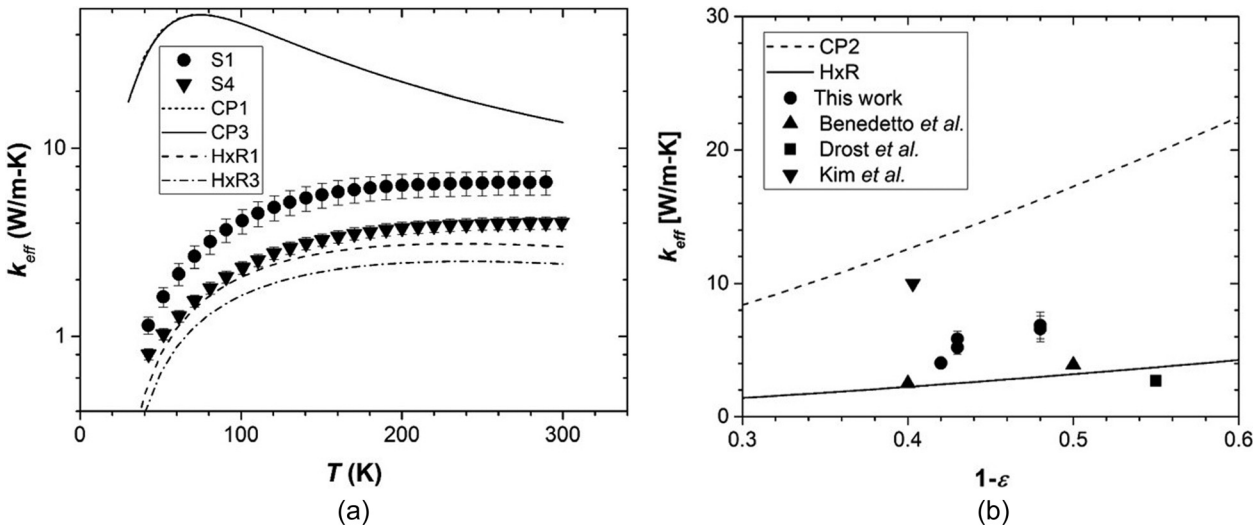

FIG. 3. Comparison of measurement results with calculations. CP and H × R denote a cylindrical pore and a hexagonally ordered round pore model, respectively, with the numbers after CP and H × R indicating the MPS film thickness in micrometers. Samples S1 and S4 have thicknesses of 1 and 3 μm, respectively. CP1 and H × R1 have a ε value of 52%, and CP2 and H × R2 have a ε value of 58%. (a) The CP model considers phonon scattering by cylindrical pores only. The boundary scattering for this model is not sufficient enough; thus, the temperature dependence differs significantly from the measurement results. The calculation results for CP1 and CP3 are almost identical. The H × R model, which incorporates the boundary scattering due to the branching pores, shows better agreement with the measurement results. (b) k_{eff} values for MPS as functions of $1-\varepsilon$ for both CP2 and H × R models. A 2-μm thickness was applied for the CP2 model. (The H × R model did not require a thickness unless the thickness specified a certain ε value.) Several measurement results are also shown. The large k_{eff} reduction in the ε range of 52%–58% (in the $1-\varepsilon$ range of 42%–48%) found in this study was not clearly explained by both the CP and H × R models together.

However, the exact phenomenon responsible for k_{eff} reduction with respect to ε remains unclear. The calculated k_{eff} value from the MPS with a ε value of 58% was only ~17 and ~19% smaller than that with a ε value of 52% based on the cylindrical and round pore models, respectively; on the other hand, the reduction of k_{eff} from the measurement results was more than ~40%. This large deviation indicates that the significant reduction of k_{eff} is not thoroughly explained by the reduction of the phonon MFPs. Other than the reduction of phonon MFPs, there are several factors, which might be influential to this phenomenon, such as phonon wave or ballistic characteristics, the morphological change of the MPSs, and elastic softening of a nanometer-thick Si structure. The ballistic or wave characteristic of phonons would not be the case; otherwise, the discrepancy among the k_{eff} values would have increased as opposed to our current observation because phonons have longer MFPs and wavelengths as temperature decreases.[7,37] Also, the constant current density and the doping concentration excluded the possibility of a significant morphological change in the MPSs. Lastly, one possible scenario for this unexpectedly large deviation is due to elastic softening, which becomes valid in sub-30-nm-thick Si and could lower the k value of approximately 5-nm-thick crystalline Si below the amorphous limit.[41,42] Notably, l' was calculated to be within the 6.0–7.4 nm range in this study, which indicates that local k_{itrs} values in the regions of the minimum characteristic size would be close to the amorphous limit of k. The Young's modulus of porous Si (E_{PS}) decreases with increasing ε, i.e., $E_{PS} \propto (1-\varepsilon)^2$,[43,44] which generates a decrease in the phonon group velocity, i.e., $v \propto \sqrt{E_{PS}}$, and accordingly a significantly large reduction in k, i.e., $k_{eff} \propto (1-\varepsilon)$ because k_{eff} is linearly proportional to v [Eq. (3)].

In summary, we measured the k_{eff} values of photoelectrochemically etched single crystalline MPS samples using the 3ω differential method. The measured k_{eff} value of 3–7 W/m-K at room temperature showed a strong dependence on the MPS ε which corresponded to the etching time. The reduced k_{eff} value was partly explained by a decrease in the phonon MFPs. The phonons were bound by the MPS skeletal structure, of which the smallest size was less than 10-nm-thick. However, the unexpectedly large k_{eff} reduction corresponding to the slight ε increase may be due to elastic softening, which reduces the local k_{itrs} value of the MPSs corresponding to the local structure sizes. This finding can be applied to tune the k_{eff} value of porous Si by a slight change in ε.

See supplementary material for details of the ε measurement via FTIR, the 3ω differential method, and the phonon MFP calculation for the cylindrical model.

This work was supported by the Basic Science Research Program through the National Research Foundation of Korea funded by the Ministry of Science, ICT & Future Planning (NRF-2014R1A1A1006148), the GIST Research Institute (GRI) in 2017, and U.S. DOE Basic Energy Sciences Energy Frontier Research Center (DoE-LMI-EFRC) under Award No. DOE DE-AC02-05CH11231.

[1]A. G. Cullis and L. T. Canham, Nature **353**(6342), 335–338 (1991).
[2]C. Biber, paper presented at the Twenty-Fourth Annual IEEE Semiconductor Thermal Measurement and Management Symposium, Semi-Therm (2008).
[3]A. I. Hochbaum, R. Chen, R. D. Delgado, W. Liang, E. C. Garnett, M. Najarian, A. Majumdar, and P. Yang, Nature **451**(7175), 163–167 (2008).
[4]H. Casimir, Physica **5**(6), 495–500 (1938).
[5]J.-K. Yu, S. Mitrovic, D. Tham, J. Varghese, and J. R. Heath, Nat. Nanotechnol. **5**, 718–721 (2010).

[6]Y. He and G. Galli, Phys. Rev. Lett. **108**(21), 215901 (2012).
[7]J. Lee, J. Lim, and P. Yang, Nano Lett. **15**(5), 3273–3279 (2015).
[8]A. Drost, P. Steiner, H. Moser, and W. Lang, Sens. Mater. **7**, 111 (1995).
[9]G. Gesele, J. Linsmeier, V. Drach, J. Fricke, and R. Arens-Fischer, J. Phys. D: Appl. Phys. **30**(21), 2911 (1997).
[10]G. Benedetto, L. Boarino, and R. Spagnolo, Appl. Phys. A **64**(2), 155–159 (1997).
[11]V. Lysenko, S. Perichon, B. Remaki, D. Barbier, and B. Champagnon, J. Appl. Phys. **86**(12), 6841–6846 (1999).
[12]J. d. Boor, D. S. Kim, X. Ao, D. Hagen, A. Cojocaru, H. Föll, and V. Schmidt, Europhys. Lett. **96**(1), 16001 (2011).
[13]K. Kim and T. E. Murphy, J. Appl. Phys. **118**(15), 154304 (2015).
[14]K. Valalaki and A. G. Nassiopoulou, J. Phys. D: Appl. Phys. **50**(19), 195302 (2017).
[15]J. D. Chung and M. Kaviany, Int. J. Heat Mass Transfer **43**(4), 521–538 (2000).
[16]Y. Chen, D. Li, J. R. Lukes, and A. Majumdar, J. Heat Transfer **127**(10), 1129–1137 (2005).
[17]R. Yang, G. Chen, and M. S. Dresselhaus, Phys. Rev. B **72**(12), 125418 (2005).
[18]F. X. Alvarez, D. Jou, and A. Sellitto, Appl. Phys. Lett. **97**(3), 033103 (2010).
[19]G. Romano, K. Esfarjani, D. A. Strubbe, D. Broido, and A. M. Kolpak, Phys. Rev. B **93**(3), 035408 (2016).
[20]Y.-C. Hua and B.-Y. Cao, Appl. Therm. Eng. **111**, 1401–1408 (2017).
[21]J.-H. Lee, G. A. Galli, and J. C. Grossman, Nano Lett. **8**(11), 3750–3754 (2008).
[22]J. Boor, D. S. Kim, X. Ao, M. Becker, N. F. Hinsche, I. Mertig, P. Zahn, and V. Schmidt, Appl. Phys. A **107**(4), 789–794 (2012).
[23]K. Valalaki, P. Benech, and A. Galiouna Nassiopoulou, Nanoscale Res. Lett. **11**(1), 201 (2016).
[24]C. C. Chiang, P. C. Juan, and T.-H. Lee, J. Electrochem. Soc. **163**(5), H265–H268 (2016).
[25]D. S. Barth, C. Gladden, A. Salandrino, K. O'Brien, Z. Ye, M. Mrejen, Y. Wang, and X. Zhang, Adv. Mater. **27**(40), 6131–6136 (2015).
[26]S. E. Foss, P. Y. Y. Kan, and T. G. Finstad, J. Appl. Phys. **97**(11), 114909 (2005).
[27]R. L. Smith and S. D. Collins, J. Appl. Phys. **71**(8), R1–R22 (1992).
[28]V. Lehmann, R. Stengl, and A. Luigart, Mater. Sci. Eng.,B **69–70**(0), 11–22 (2000).
[29]D. H. Ge, M. C. Wang, W. J. Liu, S. Qin, P. L. Yan, and J. W. Jiao, Electrochim. Acta **88**(0), 141–146 (2013).
[30]H. Föll, M. Christophersen, J. Carstensen, and G. Hasse, Mater. Sci. Eng., R **39**(4), 93–141 (2002).
[31]M. Khardani, M. Bouaïcha, and B. Bessaïs, Phys. Status Solidi C **4**(6), 1986–1990 (2007).
[32]M. Thönissen, S. Billat, M. Krüger, H. Lüth, M. G. Berger, U. Frotscher, and U. Rossow, J. Appl. Phys. **80**(5), 2990–2993 (1996).
[33]M. Park, J. Koo, J. Kim, H. Jeon, C. Bae, and C. Krug, Appl. Phys. Lett. **86**(25), 252110 (2005).
[34]P. de Rouffignac, Z. Li, and R. G. Gordon, Electrochem. Solid-State Lett. **7**(12), G306–G308 (2004).
[35]S. M. Lee, D. Cahill, and T. Allen, Phys. Rev. B **52**(1), 253–257 (1995).
[36]W. Fulkerson, J. Moore, R. Williams, R. Graves, and D. McElroy, Phys. Rev. **167**(3), 765–782 (1968).
[37]M. G. Holland, Phys. Rev. **132**(6), 2461 (1963).
[38]M. Asheghi, K. Kurabayashi, R. Kasnavi, and K. E. Goodson, J. Appl. Phys. **91**(8), 5079–5088 (2002).
[39]W. Liu and M. Asheghi, J. Heat Transfer **128**(1), 75–83 (2005).
[40]A. Majumdar, J. Heat Transfer **115**(1), 7–16 (1993).
[41]M. C. Wingert, S. Kwon, M. Hu, D. Poulikakos, J. Xiang, and R. Chen, Nano Lett. **15**(4), 2605–2611 (2015).
[42]L. Yang, Y. Yang, Q. Zhang, Y. Zhang, Y. Jiang, Z. Guan, M. Gerboth, J. Yang, Y. Chen, D. Greg Walker, T. T. Xu, and D. Li, Nanoscale **8**, 17895–17901 (2016).
[43]D. Bellet, P. Lamagnère, A. Vincent, and Y. Bréchet, J. Appl. Phys. **80**(7), 3772–3776 (1996).
[44]C. Populaire, B. Remaki, V. Lysenko, D. Barbier, H. Artmann, and T. Pannek, Appl. Phys. Lett. **83**(7), 1370–1372 (2003).